Reaction of Aldehydes with the $H_5PV_2Mo_{10}O_{40}$ Polyoxometalate and Cooxidation of Alkanes with Molecular Oxygen

Alexander M. Khenkin, Avi Rosenberger, and Ronny Neumann[1]

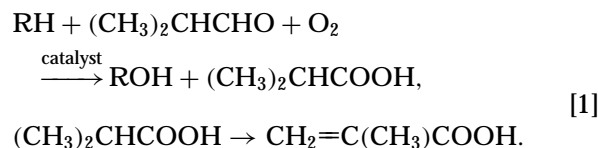*Casali Institute of Applied Chemistry, Graduate School of Applied Science, The Hebrew University of Jerusalem, Jerusalem, Israel 91904*

The oxidation of alkanes with molecular oxygen using aldehydes as reducing agents (aldehydes are cooxidized) was studied using the α-$H_5PV_2Mo_{10}O_{40}$ polyoxometalate as catalyst. Emphasis was placed on the initiation of the radical chain reaction by investigation of the aldehyde–polyoxometalate interaction. Using ^{31}P NMR and ESR spectroscopy one could differentiate between the reactivity of the five inseparable isomers of α-$H_5PV_2Mo_{10}O_{40}$. Contrary to previous belief, the 1,11 isomer with vanadium in distal positions is the most abundant. The ^{31}P NMR and ESR spectra supported by UV–vis absorption–time profiles of the reduction of α-$H_5PV_2Mo_{10}O_{40}$ indicated that isomers with vanadium in vicinal positions were most kinetically viable in the alkane oxidation. Addition of isobutyraldehyde to α-$H_5PV_2Mo_{10}O_{40}$ gave in the [51]V NMR spectrum a new downfield peak attributed to the formation of an aldehyde–polyoxometalate intermediate. The alkane/aldehyde/O_2 oxidizing system was found to be quite effective and selective for ketone formation. Reaction probes indicated that acyl peroxo radicals were the active oxidizing intermediates. Five pathways for its reaction were identified: chain propagation, alkane oxidation, decomposition to form oxygen, decomposition to acyl oxo radicals leading to CO_2 and ketone, and capture and inhibition by the polyoxometalate.   © 1999 Academic Press

Key Words: polyoxometalate; aldehyde; oxygen; alkane oxidation.

INTRODUCTION

Effective and selective oxygenation of the inactive carbon–hydrogen bonds of alkanes, ideally with molecular oxygen as oxidant, remains a fundamental research goal for chemists interested in catalysis (1–3). To achieve this goal of dioxygen activation for alkane oxidation, catalysts must be found that are selective and stable under oxidizing conditions. One particularly attractive method for catalytic oxidation of hydrocarbons with dioxygen is to use electron donors such as aldehydes (4, 5). In such systems the aldehyde is cooxidized to the corresponding carboxylic acid. Readily available isobutyraldehyde is especially attractive

since the isobutyric acid coproduct could be useful for the preparation of methacrylic acid:

$$RH + (CH_3)_2CHCHO + O_2$$
$$\xrightarrow{\text{catalyst}} ROH + (CH_3)_2CHCOOH,$$
$$(CH_3)_2CHCOOH \rightarrow CH_2{=}C(CH_3)COOH. \qquad [1]$$

From the mechanistic point of view, the intermediate product of the dioxygen reduction, the peracid and/or acyl peroxo radical, may be formed either thermally (6) or catalytically in the presence of a transition metal-based catalyst (7). Although the aldehyde/O_2 system has been very widely used and studied for alkene oxidation, there are surprisingly relatively few examples on the use of transition metal compounds as efficient catalysts for oxidation of the more inert alkanes with aldehyde/O_2 (8–13).

Polyoxometalates (POMs), known and stable catalysts for oxidation of organic compounds (14–16), also catalyze the oxidation of alkenes in the presence of aldehydes and dioxygen (17–21). A recent article (22) has convincingly shown that with transition metal-substituted polyoxometalate catalysts of the type $PMW_{11}O_{39}^{q-}$, where M is a transition metal, the reaction proceeded by a radical chain mechanisms with acyl peroxo radicals as the active species for epoxidation. Three important functions of the polyoxometalates were chain initiation by reaction of the polyoxometalate with the aldehyde, chain branching by polyoxometalate-mediated decomposition of peracids formed, and chain termination through capture of active radical species and formation of stable complexes.

Although many types of polyoxometalate-catalyzed reactions are continuously being reported (14–16), one compound that has been catalytically active in many liquid-phase reactions with molecular oxygen has been the mixed addenda phosphovanadomolybdate, α-$H_5PV_2Mo_{10}O_{40}$. An initial interaction consisting of an electron plus proton transfer from the organic substrate to the α-$H_5PV_2Mo_{10}O_{40}$ catalyst has been postulated to begin the catalytic cycle (23):

$$RH + H_5PV_2^{V}Mo_{10}O_{40} \rightarrow H_6PV^{V}V^{IV}Mo_{10}O_{40}|R^{\bullet}. \qquad [2]$$

[1] To whom correspondence should be addressed. Fax: +972-2-6528250. E-mail: Ronny@vms.huji.ac.il.
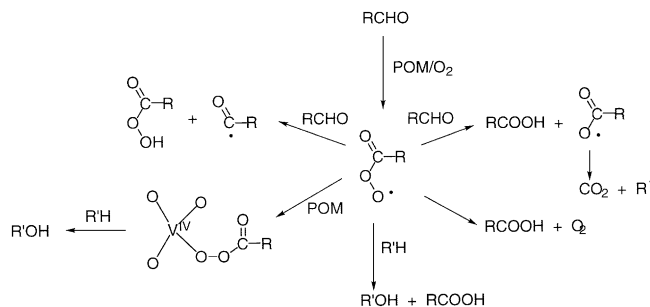
SCHEME 1

In the specific case of the cooxidation of aldehyde and alkane in the presence of dioxygen an acyl peroxo radical may be quickly formed by reaction of RCHO with α-$H_5PV_2Mo_{10}O_{40}$. Possible fates of this radical are given in generalized Scheme 1. In this paper we describe our research concerning the reaction of the α-$H_5PV_2Mo_{10}O_{40}$ polyoxometalate with aldehyde and the initiation of the complex catalytic cycle in Scheme 1. This initiation of the radical chain mechanism leads to alkane oxidation to ketones.

EXPERIMENTAL METHODS

Materials

The α-$H_5PV_2Mo_{10}O_{40}$ polyoxometalate was prepared by the standard technique and used as the hydrate after recrystallization (24). Thermogravimetric analysis (Mettler 50) indicated 32 water molecules per polyoxometalate and elementary analysis yielded the following: found (calculated) % P, 1.31 (1.34); V, 4.38 (4.41); Mo, 41.32 (41.56). This showed that the compound was in fact $H_5PV_2Mo_{10}O_{40} \cdot 32H_2O$. Solvents were of analytical grade (Frutarom) and used without further purification. Alkanes and aldehydes used in the oxidation reactions were reagent grade from Fluka and Aldrich and had purities >99% by gas chromatography (GC). Aldehydes were purified by distillation prior to use and stored under nitrogen.

Instrumentation

Oxidation reaction products were characterized using reference compounds when available by use of GLC (Hewlett–Packard 5890 gas chromatograph) with a flame ionization detector and a 15 m × 0.32 mm 5% phenylmethylsilcone (0.25-μm coating) capillary column and helium carrier gas. Products whose initial identity was questionable were unambiguously identified using a gas chromatograph equipped with a mass selective detector (GC-MS Hewlett–Packard 5970A) equipped with the same column described above.

UV–vis spectra and redox kinetic measurements were made on a Hewlett–Packard 8452A diode array spectrom-

eter. For absorption–time profiles a 1 mM solution of α-$H_5PV_2Mo_{10}O_{40}$ was prepared and the quartz cuvette was deaerated with a gentle nitrogen flow for 30 min. The temperature was regulated via a built-in bath connected to a temperature-controlled circulator. Isobutyraldehyde (25 eq) was added by syringe and measurements were initiated. For catalyst reoxidation, the reoxidation was initializing by aeration of previously reduced α-$H_5PV_2Mo_{10}O_{40}$ with oxygen. ESR spectra (X-band) were taken with a Varian E-12 spectrometer at room temperature using 10 mM α-$H_5PV_2Mo_{10}O_{40}$ in acetone; DPPH was used as standard. ^{31}P and ^{51}V NMR spectra of 10 mM α-$H_5PV_2Mo_{10}O_{40}$ in acetone-d_6 (99.5% Aldrich) were recorded at room temperature using 5-mm tubes with a Bruker DRX-400 spectrometer at 161.98 and 105.15 MHz using 85% H_3PO_4 and $VOCl_3$ as an external standards, respectively.

Procedure for Catalytic Oxidation

The progress of the reaction for the oxidation of aliphatic compounds with aldehyde/O_2 was monitored using gas chromatography. Most reactions were carried out in a 200-ml flask equipped with septum and a stirring bar. Catalyst, typically 0.1 μmol, and substrate, usually 1.5 mmol, were dissolved in 1 ml of solvent. Dioxygen was bubbled through the reaction solution for 5 min, then closed. The solution was kept at the appropriate temperature; aldehyde, typically 0.1 ml, was added by syringe, and the progress of the reaction was monitored by GC. GLC analysis was performed on aliquots withdrawn directly from the reaction mixture.

RESULTS AND DISCUSSION

Reaction initiation: The Reaction of Aldehyde with α-$H_5PV_2Mo_{10}O_{40}$

The α-$H_5PV_2Mo_{10}O_{40}$ polyoxometalate (Fig. 1) is an inseparable mixture of five isomers. A ^{31}P NMR spectrum of α-$H_5PV_2Mo_{10}O_{40}$ in acetone-d_6 is given in Fig. 2a and clearly shows that five peaks may be observed at [−3.96 (6), −3.42 (1), −3.37 (4), −3.31 (2) and −3.22 (2) ppm (area of peak)]. An additional sixth peak at −4.38 ppm is from the α-$H_5PVMo_{11}O_{40}$ impurity. First, it is interesting to note that for the first time using ^{31}P NMR spectroscopy in acetone-d_6, one can easily differentiate between the five isomers of α-$H_5PV_2Mo_{10}O_{40}$. In the past, in water as solvent, fewer peaks for α-$H_5PV_2Mo_{10}O_{40}$ were observed (25–27), although other peaks assigned to β-$H_5PV_2Mo_{10}O_{40}$ were apparently detected (27). Statistically a ratio of 2 : 2 : 2 : 4 : 1 for the 1,2; 1,4; 1,5; 1,6 and 1,11 isomers was to be expected (27, 28), but significantly this was *not* observed. Especially noteworthy is the one more intense peak at a higher field, −3.22 ppm, compared with the other four peaks at the lower field.
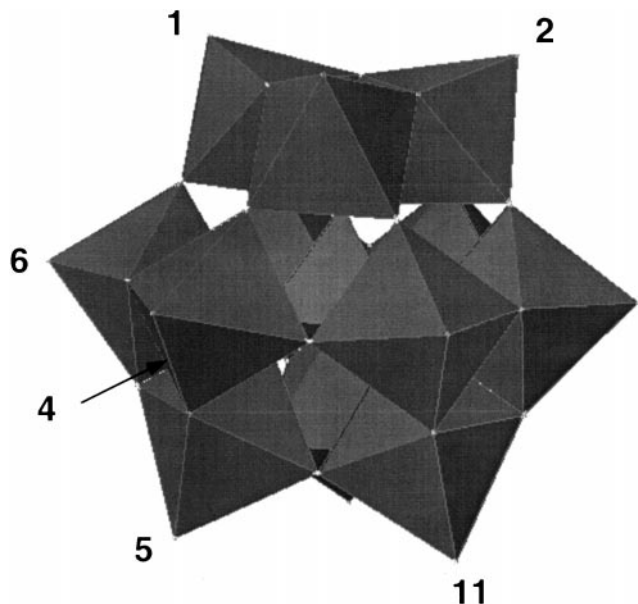
FIG. 1. Representation of the α-$H_5PV_2Mo_{10}O_{40}$ polyoxometalate and the five isomers.

To the α-$H_5PV_2Mo_{10}O_{40}$ polyoxometalate in acetone-d_6 we added 5 eq of isobutyraldehyde and kept the solution under 1 atm nitrogen for 1 h. The catalyst was slightly reduced as may be appreciated by the appearance of light green color due to the formation of the reduced heteropoly blue. A repeated ^{31}P NMR spectrum showed the same five peaks (slightly shifted due to paramagnetism) but of *different* intensities. Most notably the intensity of the high-field peak is unchanged versus the impurity peak (an internal standard) but the low-field peaks are considerably reduced in intensity (Fig. 2b). An additional measurement of the ^{31}P NMR spectra after 5 h showed almost complete disappearance of the low-field peaks. After 7 days the high-field peak also disappeared. Our explanation for these results is as follows. Although it has generally been thought (27–30) that a more or less statistical isomeric distribution of the vanadium atoms in the α-$PV_2Mo_{10}O_{40}^{5-}$ anion should be expected, in fact, it seems very conceivable that the most stable isomer would be the one with the greatest separation between the vanadium atoms, i.e., the 1,11 isomer, since increasing the number of vanadium atoms considerably destabilizes the Keggin structure. Thus, the α-$PV_4Mo_8O_{40}^{7-}$ anion has not been isolated (crystallized) and the order of stability is $PV_3Mo_9O_{40}^{6-} < PV_2Mo_{10}O_{40}^{5-} < PVMo_{11}O_{40}^{4-}$ (29, 30). Additionally, the nearer the vanadium atoms are to one another, the less even is the distribution of the negative charge on the polyanion, therefore reasonably causing destabilization. The ^{31}P NMR spectra in Fig. 2 seem to support this conclusion. The position of the higher-field peak of the 1,11 α-$PV_2Mo_{10}O_{40}^{5-}$ isomer versus the other α-$PV_2Mo_{10}O_{40}^{5-}$ isomers is to be expected since the order in the ^{31}P NMR absorption (high field to low field) is α-$PMo_{12}O_{40}^{3-} >$

α-$PVMo_{11}O_{40}^{4-} > \alpha$-$PV_2Mo_{10}O_{40}^{5-} > \alpha$-$PV_3Mo_9O_{40}^{6-}$ (27, 28). Furthermore, we have already shown in the past (23) that redox interactions between α-$PV_2Mo_{10}O_{40}^{5-}$ and organic substrates are to be preferred at vicinal vanadium positions (see also ESR experiment below) and other computational and experimental information supports this conclusion (31, 32). Thus, initially in the slightly reduced sample (Fig. 2b), the reduced intensity of the four peaks at the lower field can easily be explained by the preferred formation of the paramagnetic α-$PV^{IV}V^VMo_{10}O_{40}^{6-}$ species with vanadium in vicinal positions which would be NMR silent due to peak broadening. The higher-field 1,11 isomer is unaffected and remains unchanged in the ^{31}P NMR. It is also important to add that the high lability of α-$PV_2Mo_{10}O_{40}^{5-}$ observed
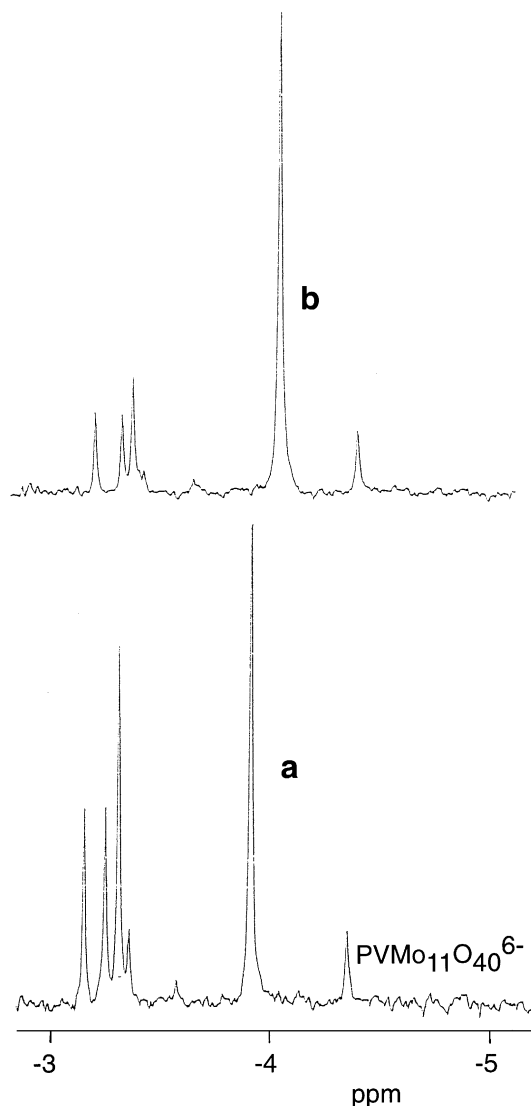

FIG. 2. ^{31}P NMR spectrum of α-$H_5PV_2Mo_{10}O_{40}$ in acetone-d_6. (a) spectrum 10 mM $H_5PV_2Mo_{10}O_{40}$ prior to addition of isobutyraldehyde. No reduction of the polyoxometalate was discernable (UV-vis). (b) spectrum one hour after addition of 5 equivalents of isobutyraldehyde under nitrogen.
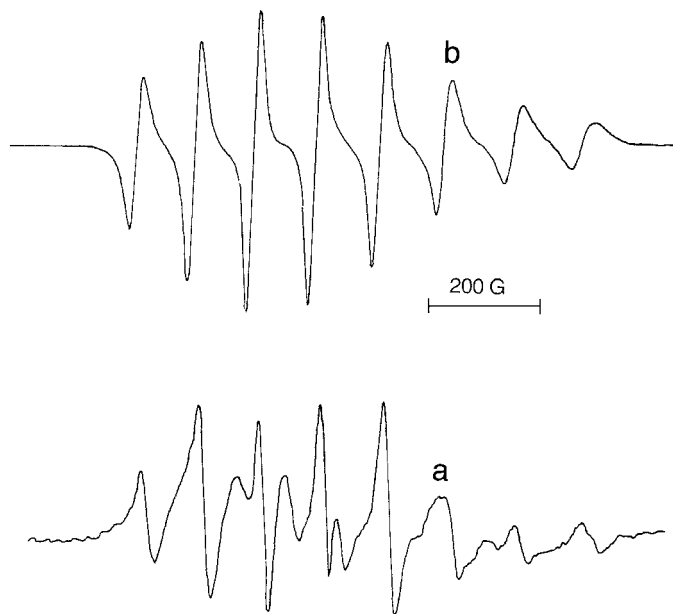
FIG. 3. ESR of α-H$_5$PV$_2$Mo$_{10}$O$_{40}$ on addition of isobutyraldehyde under N$_2$. The ESR spectrum was of a 10 mM H$_5$PV$_2$Mo$_{10}$O$_{40}$ solution in acetone after addition of 5 eq isobutyraldehyde under nitrogen at ambient temperature. Microwave power = 50 mW, frequency = 9.48 GHz, modulation = 5 G. (a) One hour after addition of isobutyraldehyde. (b) Five days after addition of isobutyraldehyde.

in aqueous solution is very significantly repressed in nonaqueous solvents because of the considerably lowered solubility of the VO^{2+} unit. Thus, little equilibration between isomers on the experiment time scale (hours) was expected and none was observed.

Parallel with the ^{31}P NMR experiment similar measurements were made using ESR spectroscopy. Prior to addition of isobutyraldehyde, α-H$_5$PV$_2$Mo$_{10}$O$_{40}$ is ESR silent. Addition of 5 eq of isobutyraldehyde under nitrogen yields a 15-line spectrum after 1 h (Fig. 3a). On the other hand, re-

measurement of the ESR spectra after several days yields a different 8-line spectrum (Fig. 3b). In line with the explanation given above, the isobutyraldehyde preferentially reacted with the vicinal isomers of α-H$_5$PV$_2$Mo$_{10}$O$_{40}$ and first a mono-reduced polyoxometalate was formed. This leads to the observation of a 15-line spectrum due to additional splitting of the 8 lines at the V^{IV} center ($I = 7/2$ for ^{51}V) by a nearest-neighbor vanadium atom in the 1,2 and 1,6 configurations. As the reduction of the polyoxometalate mixture continues, the 1,2 and 1,6 isomers become doubly reduced, and because of antiferromagnetic coupling these isomers become ESR silent. The slower reduction of the more distal isomeric forms, especially the 1,11 isomer, leads to a simple 8-line spectrum with no nearest-neighbor interaction.

Although both the ^{31}P NMR and ESR experiments described above clearly indicated different reactivity of isobutyraldehyde with different isomers of α-H$_5$PV$_2$Mo$_{10}$O$_{40}$, we sought more information on this reaction. The reduction of α-H$_5$PV$_2$Mo$_{10}$O$_{40}$ can be monitored by UV–vis spectroscopy at 750 nm. Thus, a profile of the reaction of 1 mM α-H$_5$PV$_2$Mo$_{10}$O$_{40}$ in acetonitrile at 26°C under nitrogen with 25 eq isobutyraldehyde (Fig. 4a) shows complex behavior. There is an initial relatively fast increase in optical density from 0 to $\sim$0.5 over a period of $\sim$15,000 s (4 h) with an approximate first-order behavior. Additional slower reduction ($\sim$0.5 to $\sim$1.0), again with an approximate first-order behavior, occurs over the following 20 h. Finally there is an even slower reduction to an optical density of 1.2 over the following 3 days. In the reoxidation reaction (at 1 atm O$_2$) of the fully reduced polyoxometalate (Fig. 4b), again three different segments in the reoxidation reaction may also be observed. At an identical concentration of α-H$_5$PV$_2$Mo$_{10}$O$_{40}$, the addition of 25 eq valeraldehyde under nitrogen instead of isobutyraldehyde leads to an increase in the optical density of 0.45 within 7 h, with no further reduction of α-H$_5$PV$_2$Mo$_{10}$O$_{40}$ thereafter (Fig. 4c). Since
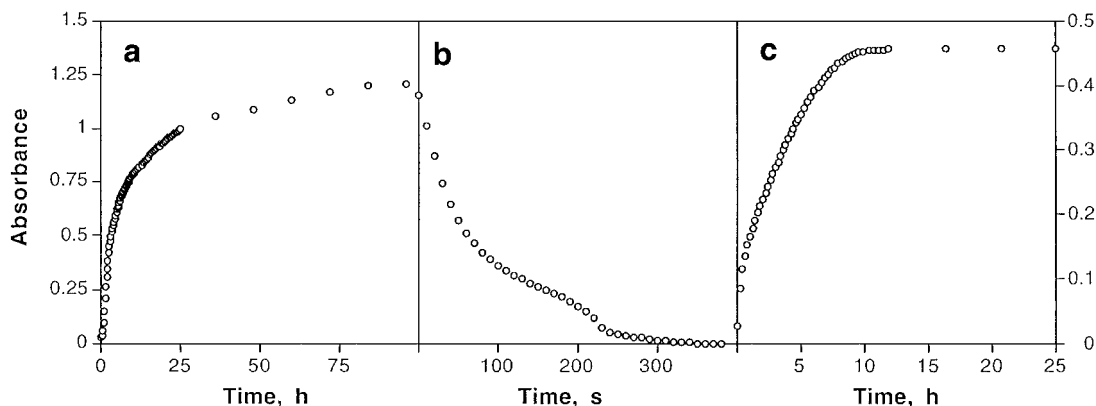
FIG. 4. Absorption–time curves of α-H$_5$PV$_2$Mo$_{10}$O$_{40}$. Absorption of α-H$_5$PV$_2$Mo$_{10}$O$_{40}$ was measured at 750 nm at 26°C. (a) Reduction of 1 mM α-H$_5$PV$_2$Mo$_{10}$O$_{40}$ in acetonitrile on addition of 25 eq isobutyraldehyde. (b) Reoxidation of reduced α-H$_5$PV$_2$Mo$_{10}$O$_{40}$ under 1 atm dioxygen. The sample was reduced by addition of 25 eq of isobutyraldehyde under nitrogen for 5 days. (c) Reduction of 1 mM α-H$_5$PV$_2$Mo$_{10}$O$_{40}$ in acetonitrile on addition of 25 eq valeraldehyde.

the isomeric mixture of α-$H_5PV_2Mo_{10}O_{40}$ is only approximately defined, it would be overly presumptuous to exactly define which reaction is occurring in each segment of the kinetic profile, but to a reasonable degree of confidence, the first segment is mostly clearly connected with mono-reduction of the more reactive vicinal isomers. The intermediate and third segments are attributed to a combination of di-reduction of the vicinal and mono-reduction of the more distal isomers. The less reactive valeraldehyde apparently leads only to reduction of the more reactive isomers and, thus, to a lesser total increase in the optical density.

The reaction of the aldehyde with the more reactive α-$H_5PV_2Mo_{10}O_{40}$ isomers is the only one of relevance in a catalytic cycle since the dioxygen will react quickly with acyl radicals formed to yield initial acyl peroxo intermediates. Propagation of this species in the autooxidation chain reaction will lead also to oxidation of the reduced polyoxometalate and only oxidized α-$H_5PV_2Mo_{10}O_{40}$ in the steady state. Indeed under alkane oxidation turnover conditions, the α-$H_5PV_2Mo_{10}O_{40}$ is always in the oxidized state. Using the method of initial rates the reaction of isobutyraldehyde with the reactive isomers of α-$H_5PV_2Mo_{10}O_{40}$ may be studied under an inert nitrogen atmosphere at different temperatures (Fig. 5). The *initial* slope is related to the reaction of isobutyraldehyde with the most reactive isomer(s) of α-$H_5PV_2Mo_{10}O_{40}$. As stated above, once the most reactive isomer(s) is reduced, isobutyraldehyde then continues to react with less reactive isomer(s) and the slope or reaction

rate decreases. As the temperature is lowered, the reaction rate is decreased and, on the time scale measured, shows increased contribution of the reaction of isobutyraldehyde with the most reactive α-$H_5PV_2Mo_{10}O_{40}$ isomer. Thus, at 10°C the curve is fairly flat, while at high temperatures there is more curvature due to consecutive reaction of isobutyraldehyde with isomers of decreasing reactivity. A further Arrhenius plot of the initial rate constants as a function of temperature (Fig. 5, inset) yields a surprisingly high activation energy of 22 kcal/mol ($\Delta H^{\ddagger}_{25°C} = 21.4$ kcal/mol, $\Delta S^{\ddagger}_{25°C} = -24$ e.u.).

To gain further understanding of the $PV_2Mo_{10}O_{40}^{5-}$–isobutyraldehyde reaction further studies were carried out using ^{51}V NMR spectroscopy (Fig. 6). Interestingly, the ^{51}V NMR spectrum of $H_5PV_2Mo_{10}O_{40}$ in acetone-d_6 was not well resolved (Fig. 6a), as opposed to the ^{31}P NMR spectrum with only two distinct peaks at −525.4 and −534.6 ppm. On addition of 5 eq of isobutyraldehyde under N_2 a new spectrum was measured after 1 h (Fig. 6b). At least one additional peak was observed downfield at −521.1 ppm. The small magnitude of the downfield shift indicates that this peak is attributable to a complex between a vanadium atom in α-$H_5PV_2Mo_{10}O_{40}$ and isobutyraldehyde. Such complexes between aldehydes and polyoxometalates have already been described and investigated in the past. It has been shown that dioxymethylene moieties are formed on the polyoxometalate (33), leading to formulation of metal acetal or hemiacetal compound, MO–OHCR (34, 35). The
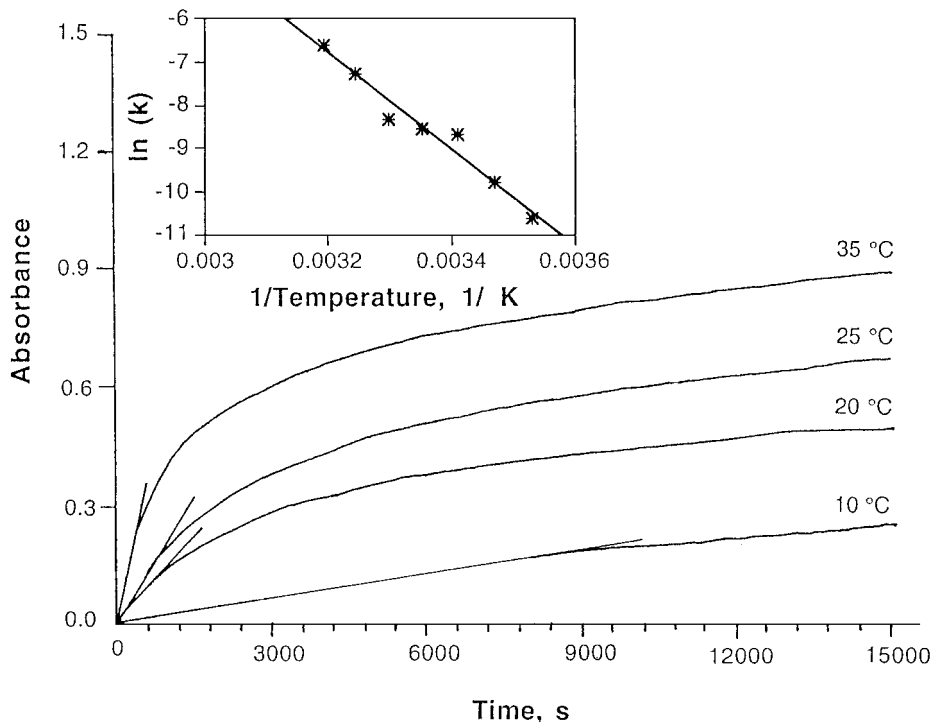

FIG. 5. Absorption–time curves for α-$H_5PV_2Mo_{10}O_{40}$ reduction as a function of temperature. Measurements were at 750 nm for 1 mM α-$H_5PV_2Mo_{10}O_{40}$ in acetonitrile reduced on addition of 25 eq isobutyraldehyde, 15–40°C. The inset is the Ahrrenius plot derived from the initial rates.

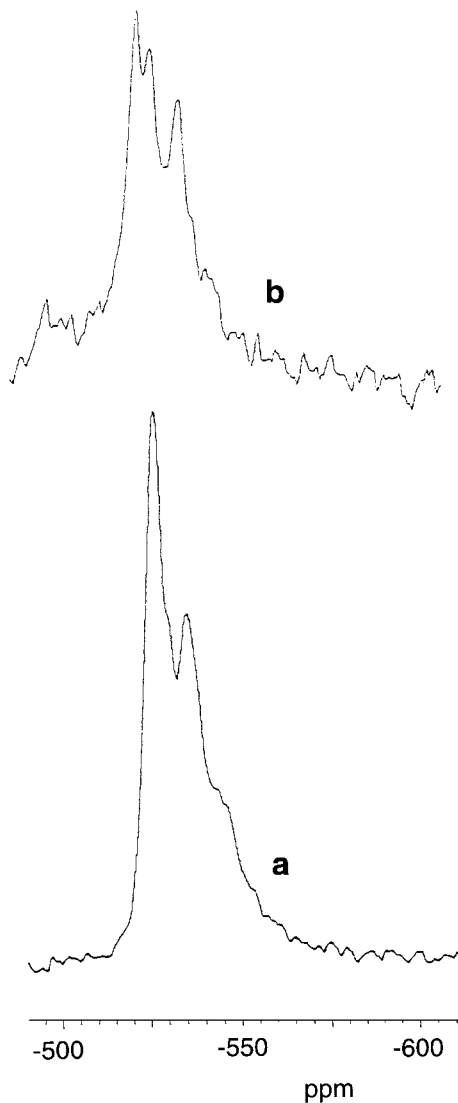**FIG. 6.** ^{51}V NMR spectra of α-H$_5$PV$_2$Mo$_{10}$O$_{40}$ in acetone-d_6. (a) Spectrum of 10 mM α-H$_5$PV$_2$Mo$_{10}$O$_{40}$ in acetone. (b) Spectrum after addition of 5 eq of isobutyraldehyde under N$_2$.

hemiacetal or acetal formation is acid catalyzed, and indeed, use of α-Q$_5$PV$_2$Mo$_{10}$O$_{40}$ ($Q = n$-Bu$_4$N) in place of α-H$_5$PV$_2$Mo$_{10}$O$_{40}$ yielded no reaction, i.e., polyoxometalate reduction with isobutyraldehyde. Further attempts to isolate (crystallize) an intermediate complex were unsuccessful.

Alkane and Aldehyde Cooxidation Initiated by α-H$_5$PV$_2$Mo$_{10}$O$_{40}$

After investigating the reaction of isobutyraldehyde with α-H$_5$PV$_2$Mo$_{10}$O$_{40}$, the initiation step for the formation of an acyl peroxo radical as the assumed active oxidizing species for the cooxidation of alkanes, we looked at the kinetic profiles of alkane oxidation in the reaction cyclooctane/aldehyde/O$_2$/α-H$_5$PV$_2$Mo$_{10}$O$_{40}$ (Fig. 7):
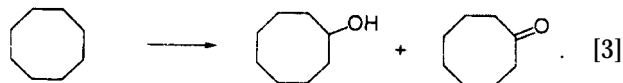
The reaction profiles showed that for isobutyraldehyde and pivaldehyde there was little to no induction period for the oxidation of cyclooctane and the reaction profile showed asymptotic behavior. Reactions (not shown) were approximately first order in cyclooctane. On the other hand, for valeraldehyde and benzaldehyde there were significant induction periods of 5–6 h and approximately linear reaction profiles, with measurably and slightly higher conversions after 24 h. Reactions were approximately zero order in cyclooctane. Control reactions showed that in the absence of α-H$_5$PV$_2$Mo$_{10}$O$_{40}$ no reaction occurred within 24 h, implying longer induction periods for non-polyoxometalate-catalyzed reactions. Importantly, there was no simple correlation between the induction period observed, cyclooctane conversion, reaction profiles, and the reduction of α-H$_5$PV$_2$Mo$_{10}$O$_{40}$ with the various aldehydes under nitrogen. Thus, both valeraldehyde and isobutyraldehyde reduced α-H$_5$PV$_2$Mo$_{10}$O$_{40}$ at ambient temperatures although to different degrees (Fig. 4), whereas for benzaldehyde and pivaldehyde no such reduction was observable. For example, mixing a 1 mM solution of α-H$_5$PV$_2$Mo$_{10}$O$_{40}$ in acetonitrile with 25 eq of benzaldehyde or pivaldehyde showed no sign of polyoxometalate reduction over a period of 10 days. Since oxidation of cyclooctane will be sustained by the autooxidation–propagation cycle, only *small* initial concentrations of an acyl radical must be attained via reaction of the aldehyde with the polyoxometalate. A reaction sequence to describe this reactivity is
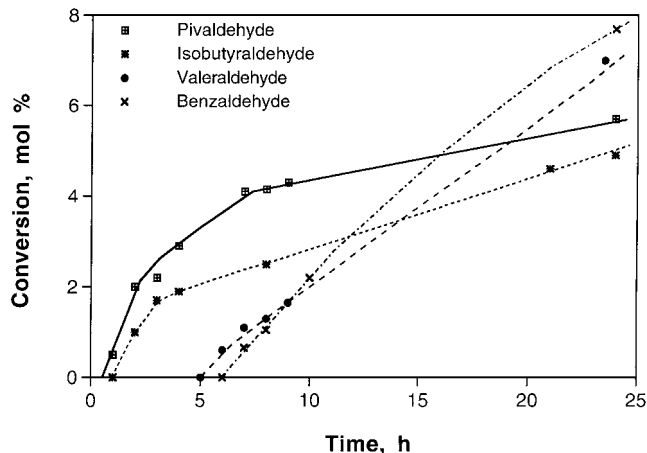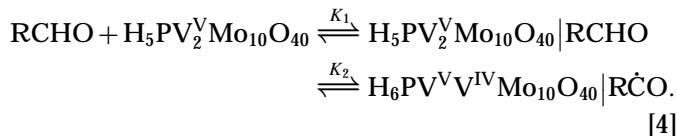
$$\text{RCHO} + \text{H}_5\text{PV}_2^{\text{V}}\text{Mo}_{10}\text{O}_{40} \underset{}{\overset{K_1}{\rightleftharpoons}} \text{H}_5\text{PV}_2^{\text{V}}\text{Mo}_{10}\text{O}_{40}|\text{RCHO}$$

$$\overset{K_2}{\rightleftharpoons} \text{H}_6\text{PV}^{\text{V}}\text{V}^{\text{IV}}\text{Mo}_{10}\text{O}_{40}|\text{R}\dot{\text{C}}\text{O}. \quad [4]$$

FIG. 7. Reaction profiles for cyclooctane cooxidation catalyzed by α-H$_5$PV$_2$Mo$_{10}$O$_{40}$. Reaction conditions: 1.0 μmol α-H$_5$PV$_2$Mo$_{10}$O$_{40}$, 1.5 mmol alkane, 1.1 mmol isobutyraldehyde in 1 ml acetic acid, $T = 25°$C.

It seems apparent from the results described above that for each aldehyde the values of K_1 and K_2 are different, leading to different reaction profiles.

The synthetic utility of the alkane oxidation is demonstrated in Fig. 8. Semicontinuous addition of isobutyraldehyde to an alkane yielded an increasing amount of product, depending only on the amount of aldehyde added. In this manner high yields of cyclooctanone were obtained from cyclooctane at 95% selectivity. Cyclohexane (not shown) was similarly reactive and yielded cyclohexanone at a greater than 99% selectivity. Acetophenone is formed almost exclusively from ethylbenzene with about 1–2 mol% phenolic products. Adamantane forms 1-adamantanol and 2-adamantanone in a 45:1 product ratio. Acyclic alkanes (not shown) such as n-octane can also be oxidized to a mixture of products although the productivity in terms of isobutyraldehyde is quite low, <3%. Somewhat surprisingly it appeared from Fig. 8 that ethylbenzene was less reactive than cyclooctane. We attributed this result to inhibition of the reaction by the small amounts of phenols formed during the reaction. Indeed, in a competitive oxidation of cyclooctane and ethylbenzene (Fig. 8, inset), one may observe that ethylbenzene is intrinsically more reactive.

Although a complete kinetic analysis was not carried out for the cyclooctane/isobutyraldehyde/O_2 cooxidation reaction, the reaction as a function of temperature yielded an activation energy $E_{a(obsd)}$ of 13.2 kcal/mol. The observed activation energy was computed from an Arrhenius plot of six initial rates found from reactions carried out at temperatures between 298 and 345 K. The other reaction conditions were 1 μmol α-$H_5PV_2Mo_{10}O_{40}$, 1.5 mmol cyclooctane, 1.1 mmol isobutyraldehyde, and 1 ml acetone. One may note that this activation energy is significantly *lower* than the activation energy found above in the re-
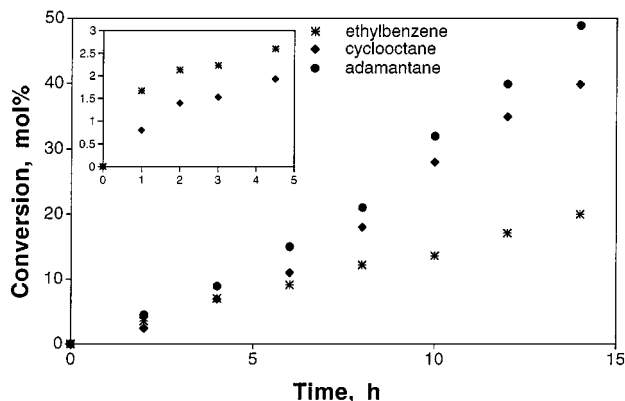

FIG. 9. Initial reaction rate as a function of the concentration of α-$H_5PV_2Mo_{10}O_{40}$. Reaction conditions: 0–10 μmol α-$H_5PV_2Mo_{10}O_{40}$, 1.5 mmol cyclooctane, 1.1 mmol isobutyraldehyde in 1 ml acetone, $T=$ 22°C.

action initiation stage, polyoxometalate–isobutyraldehyde $E_a = 21.4$ kcal/mol. This of course strongly supports other evidence presented below that the polyoxometalate is not directly involved in the alkane oxidation, but rather initiates formation of the oxidatively active acyl peroxo radical. In the past (22) it was shown that the polyoxometalate catalyst also may inhibit the autooxidation reaction. For α-$H_5PV_2Mo_{10}O_{40}$ the dependence on reaction rate in the $H_5PV_2Mo_{10}O_{40}$ catalyst concentration is given in Fig. 9. There is a clear deceleration of the reaction rate at higher catalyst concentrations. Thus, maximum rates are observed at a catalyst:substrate ratio of 1:1000 although the turnover frequency and productivity of isobutyraldehyde are highest at ratios of approximately 1:10,000. At a higher catalyst:substrate ratio of 1:100 there is a fivefold decrease in rate accompanied by a decrease in the productivity of the isobutyraldehyde leading to cyclooctanone and also of course a lower cyclooctane conversion. It is well worth pointing out that when using benzaldehyde instead of isobutyraldehyde as cooxidant the reaction is almost totally inhibited by the catalyst at a 1:100 $H_5PV_2Mo_{10}O_{40}$:benzaldehyde ratio. This is in line with our previous finding (36) that the autooxidation of benzaldehyde is inhibited by $H_5PV_2Mo_{10}O_{40}$ and the finding of Ishii and his co-workers (17) that benzaldehyde was inactive as cooxidant for the epoxidation of 2-octene with $(NH_4)_5H_4PV_6Mo_6O_{40}$.

During the course of alkane oxidation there is significant nonproductive oxidation of isobutyraldehyde. A material balance on the fate of isobutyraldehyde was therefore studied under turnover conditions. A full mass balance of a cyclooctane oxidation carried out in MIBK as solvent at a $H_5PV_2Mo_{10}O_{40}$:isobutyraldehyde:cyclooctane ratio of 1:1100:1500 at ambient temperature showed that 91 mol% isobutyraldehyde had reacted after 5 h. Thus, a reaction of 7.5 mmol cyclooctane and 5.5 mmol isobutyraldehyde under 1 atm of O_2 in the presence of 5 μmol $H_5PV_2Mo_{10}O_{40}$

FIG. 8. Reaction profiles for the oxidation of alkanes with semicontinuous addition of isobutyraldehyde. Reaction conditions: 0.1 μmol α-$H_5PV_2Mo_{10}O_{40}$, 1.5 mmol alkane, 1.1 mmol isobutyraldehyde added every 2 h in 1 ml acetic acid, $T=22$°C. The inset is a reaction profile of a competitive reaction between cyclooctane (0.75 mmol) and ethylbenzene (0.75 mmol) with the addition of 1.1 mmol isobutyraldehyde.
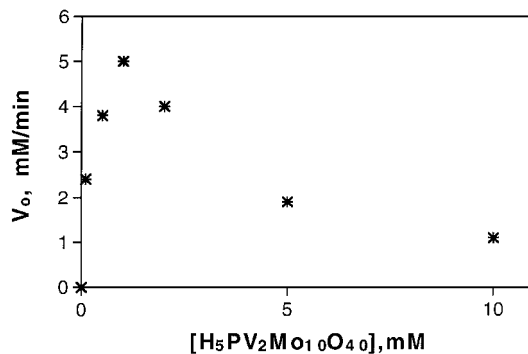
in 5 ml of MIBK yielded, as determined by GLC, 7.1 mmol of cyclooctane, 0.4 mmol of cyclooctanone/cyclooctanol, 0.5 mmol of isobutyraldehyde, 4.4 mmol of isobutyric acid, 0.6 mmol of acetone, and 0.5 mmol of CO$_2$ (determined as BaCO$_3$). This result shows that approximately 16% of the reacted isobutyraldehyde is used to form a cyclooctane oxidation product and isobutyric acid as coproduct, 72% is oxidized to isobutyric acid without oxidation of cyclooctane, and 12% is decomposed to acetone and CO$_2$. The various pathways explaining the fate of isobutyraldehyde are discussed below.

Although it was assumed above and suggested in the past that the active oxidant in hydrocarbon/aldehyde/O$_2$ systems is the acyl peroxo radical, supporting evidence for this conclusion was sought with the cooxidation studied here. The first useful probe was adamantane as substrate since the ratio of oxidation products at tertiary versus secondary carbons is often used as a mechanistic probe. Oxidation under standard conditions of adamantane (1500) with H$_5$PV$_2$Mo$_{10}$O$_{40}$ (1) : isobutyraldehyde (1100) : O$_2$ (1 atm) in acetone yielded only 1-adamantanol and 2-adamantanone at a ratio of $4.5 \pm 0.5 : 1$. This ratio is significantly higher than the ratio found (2–2.5 : 1 for metal-catalyzed autooxidation of adamantane with only molecular oxygen (no aldehyde) (37). Therefore, apparently, the alkane radical intermediate is formed by reaction with a radical derived from the aldehyde rather than direct alkane activation by the catalyst. This deduction was strengthened by the observation that the oxidation of 1,3-adamantane-d_2 yielded an internal kinetic isotope effect of 4.3 ± 0.2 for formation 1-adamantanol, similar to the value obtained in oxidation with a t-butoxy radical (38), compared with a value of ~2 measured for metal-catalyzed autooxidation. The latter value was obtained by by oxidizing 1,3-adamantane-d_2 with 1 atm dioxygen at 80°C using 0.1 mol% Q_5PCoW$_{11}$O$_{39}$ (Q = tetrahexylammonium) as catalyst. For comparison an acyl peroxo radical, CH$_3$C(O)OO•, was generated by the reaction of potassium superoxide with acetyl chloride (39). Thus, adamantane was oxidized to 1-adamantanol (80%), 2-adamantanol (18.4%), and 2-adamantanone (1.6%) with regioselectivity very similar to what was found for H$_5$PV$_2$Mo$_{10}$O$_{40}$/isobutyraldehyde/O$_2$. The product selectivity of the oxidation of the secondary carbon was, however, considerably different with 2-adamantanol as major product and only little 2-adamantanone. Since these results were equivocal further probe substrates were examined.

Further information was gathered by oxidizing *cis*-1,2-dimethylcyclohexane,

[5]
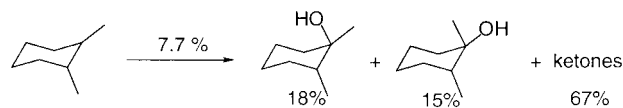
and *cis*- or *trans*-decalin,

[6]
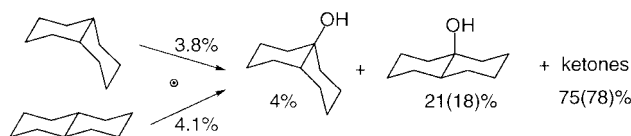
in acetone under standard conditions as described in Fig. 7. In all cases thermodynamic mixtures of *cis* and *trans* tertiary alcohols were formed without retention of configuration. Clearly, the reaction probes provided a very good indication for formation of a acyl peroxo intermediate in the catalytic cycle (40, 41). Thus, the results of the oxidation of various probe alkanes point to the likely certainty that the acyl peroxo radical is the major and perhaps only operative oxidant in the alkane oxidation. The different 2-adamantanol/2-adamantanone ratios found in the PV$_2$Mo$_{10}$O$_{40}^{5-}$/IBA/O$_2$ versus the CH$_3$COCl/KO$_2$ systems and the high ketone/alcohol ratio found in general for the cyclohexane, cyclooctane, and ethylbenzene oxidation reactions as compared with other results obtained in other systems (8–13) are attributed to the known acid-catalyzed decomposition of the intermediate hydroperoxide to ketone (42–44). Additionally, comparison of the rate of cyclooctanol ($V_0 = 2.0$ μmol/min) versus cyclooctane ($V_0 = 2.4$ μmol/min) oxidation clearly indicates that the rate for oxidation of the former is insufficient to explain the ketone/alcohol ratio that was observed. Thus, it would appear that while the acyl peroxo radical is propagated in a radical chain reaction, the oxidation of the alkane is mostly terminated by acid-catalyzed formation of the ketone from the alkyl hydroperoxide once the latter is formed as intermediate (42).

As noted in the Introduction (Scheme 1), once a free acyl peroxo radical is formed then in general there are five possible pathways for its reaction. One pathway leads to cooxidation of the alkane. The second pathway is reaction with more aldehyde to propagate a free radical chain to form more acyl radicals and isobutyric peracid. The peracid may of course be decomposed by the polyoxometalate in the typical Haber–Weiss process. Evidence for its formation was obtained by using thianthrene oxide as a probe since it has been used to test whether an electrophilic oxidant, e.g., peracid, is present in a reaction system (45, 46). A pure acetyl peroxo radical prepared as above from KO$_2$ and acetyl chloride did not oxidize thianthrene oxide. However, oxidation with aldehyde/O$_2$ under standard conditions led to 60% conversion and formation of thianthrene 5,10-dioxide (71%) as major product and thianthrene 5,5-dioxide (12%) and thianthrene 5,5,10-trioxide (17%) as minor products. One may conclude that an electrophilic oxidant, e.g., isobutyric peracid, is also formed. Isobutyric peracid was inactive in alkane oxidation as proven by the finding that when equivalent amounts of isobutyric peracid

and cyclooctane in acetone were mixed no product was formed.

The third pathway is for the acyl peroxo radical to react with aldehyde to form an acyl oxo radical and carboxylic acid. The acyl oxo radical can then he decomposed to CO_2 and acetone (via the alkyl radical and dioxygen in the presence of acid) (42). We have already described above the experiment showing that indeed about $\sim$10–12% of the aldehyde eventually decomposes to acetone and CO_2. In the fourth pathway, two peroxo radicals may combine to form oxygen and acid. The existence of this pathway may be inferred in so much as $\sim$70% of isobutyraldehyde was nonproductively decomposed. In the final pathway, the acyl peroxo radical could react with a vanadium (molybdenum) center in the polyoxometalate to yield a vanadium-centered peroxo species. The intermediacy of a polyoxometalate peroxo compound POM–O–O–C(O)CH(CH$_3$)$_2$ was more difficult to prove conclusively. Its formation may, however, be inferred from the inhibition of the alkane oxidation at high $H_5PV_2Mo_{10}O_{40}$ concentrations. The $H_5PV_2Mo_{10}O_{40}$ compound, although catalyzing formation of the acyl peroxo radical on the one hand, also then captures the active acyl peroxo radical, effectively inhibiting the radical chain reaction (22) (Fig. 9). The steady-state concentration of the expected POM–O–O–C(O)CH(CH$_3$)$_2$ intermediate is, however, very low for the addition of oxygen to an NMR tube containing $H_5PV_2Mo_{10}O_{40}$ and isobutyraldehyde at a 1-to-20 ratio showed no downfield shifted peak attributable to a vanado–peroxo species at $\sim$−650–750 ppm (47, 48).

CONCLUSION

The initiation of alkane/aldehyde cooxidation with dioxygen and the α-$H_5PV_2Mo_{10}O_{40}$ polyoxometalate as catalyst has been investigated. ^{31}P NMR and ESR measurements showed that the various isomers of α-$H_5PV_2Mo_{10}O_{40}$ have different reactivities toward isobutyraldehyde. Analysis of the spectra indicated that isomers with vanadium atoms in vicinal positions are most reactive toward aldehyde. The UV–vis-derived kinetic profiles of the aldehyde/POM interaction under nitrogen showing various aldehyde/POM reaction regimes support the concept of different reactivity for different isomers. In the presence of oxygen, the polyoxometalate is always in the oxidized state and therefore only the vicinal isomers are viable in the alkane cooxidation reaction. From the ^{51}V NMR spectrum it was learned that an aldehyde–POM complex was formed. Although initial acyl radical formation is of high activation energy, once formed even in small amounts, the cyclooctane oxidation is propagated through a radical chain autooxidation mechanism. Reaction probes and material balance support an acyl peroxo radical as active oxidizing species for alkane oxidation. The α-$H_5PV_2Mo_{10}O_{40}$ compound also inhibits the oxidation reaction presumably due to capture of the active acyl peroxo radical intermediate.

REFERENCES

1. Hill, C. L., "Activation and Functionalization of Alkanes." Wiley, New York, 1989.
2. Shilov, A. E., "Activation of Saturated Hydrocarbons by Transition Metal Complexes." Reidel, Dordrecht, 1984.
3. Barton, D. H. R., and Doller, D., *Acc. Chem. Res.* **25**, 504 (1992).
4. Landau, R., Sullivan, G. A., and Brown, D., *Chemtech*, 602 (1979).
5. Mukaiyama, T., and Yamada, T., *Bull. Chem. Soc. Jpn.* **68**, 17 (1995).
6. Filippova, T. V., and Blyumberg, E. A., *Russ. Chem. Rev.* **51**, 582 (1982).
7. Nam, W., Kim, H. J., Kim, S. H., Ho, R. Y. N., and Valentine, J. S., *Inorg. Chem.* **35**, 1045 (1996).
8. Murahashi, S.-I., Oda, Y., and Naota, T., *J. Am. Chem. Soc.* **114**, 7913 (1992).
9. Murahashi, S.-I., Oda, Y., Naota, T., and Komiya, N., *J. Chem. Soc. Chem. Comun.*, 139 (1993).
10. Murahashi, S.-I., Naota, T., and Komiya, N., *Tetrahedron Lett.* **36**, 8059 (1995).
11. Komiya, N., Naota, T., and Murahashi, S.-I., *Tetrahedron Lett.* **37**, 1633 (1996).
12. Mastrorilli, P., and Nobile, C. F., *Tetrahedron Lett.* **35**, 4193 (1994).
13. Punniyamurthy, T., Kalra, S. J. S., and Iqbal, J., *Tetrahedron Lett.* **36**, 8497 (1995).
14. Hill, C. L., and Prosser-McCartha, C. M., *Coord. Chem. Rev.* **143**, 407 (1995).
15. Okuhara, T., Mizuno, N., and Misono, M., *Adv. Catal.* **41**, 113 (1996).
16. Neumann, R., *Prog. Inorg. Chem.* **47**, 317 (1998).
17. Hamamoto, M., Nakayama, K., Nishiyama, Y., and Ishii, Y., *J. Org. Chem.* **58**, 6421 (1993).
18. Mizuno, N., Hirose, T., Tateishi, M., and Iwamoto, M., *Chem. Lett.*, 1839 (1993).
19. Mizuno, N., Tateishi, M., Hirose, T., and Iwamoto, M., *Chem. Lett.*, 1985 (1993).
20. Mizuno, N., Hirose, T., Tateishi, M., and Iwamoto, M., *Stud. Surf. Sci. Catal.* **82**, 593 (1994).
21. Mizuno, N., Weiner, H., and Finke, R. G., *J. Mol. Catal.* **114**, 15 (1996).
22. Kholdeeva, O. A., Grigoriev, V. A., Maksimov, G. M., Fedotov, M. A., Golovin, A. V., and Zamaraev, K. I., *J. Mol. Catal.* **114**, 123 (1996).
23. Neumann, R., and Levin, M., *J. Am. Chem. Soc.* **114**, 7278 (1992).
24. Tsigdinos, G. A., and Hallada, C. J., *Inorg. Chem.* **7**, 437 (1968).
25. Pope, M. T., O'Donnell, S. E., and Prados, R. A., *J. Chem. Soc. Chem. Commun.*, 22 (1975).
26. O'Donnell, S. E., and Pope, M. T., *J. Chem. Soc. Dalton Trans.*, 2290 (1976).
27. Pettersson, L., Andersson, I., Selling, A., and Grate, J. H., *Inorg. Chem.* **33**, 982 (1994).
28. Pope, M. T., O'Donnell, S. E., and Prados, R. A., *Adv. Chem.* **150**, 85 (1976).
29. Kozhevnikov, I. V., and Matveev, K. I., *Appl. Catal.* **5**, 135 (1983).
30. Pope, M. T., "Heteropoly and Isopoly Oxometalates." Springer, New York, 1983.
31. Yurchenko, E. N., Miessner, H., and Trunschke, A., *J. Struct. Chem. (Engl. Trans.)* **30**, 22 (1989).
32. Klemperer, W., and Shum, G., *J. Am. Chem. Soc.* **100**, 4891 (1978).
33. Popova, G. A., Budneva, A. A., and Andrushkevich, T. V., *React. Kinet. Catal. Lett.* **61**, 353 (1997).

34. Misono, M., Sakata, K., Yoneda, Y., and Lee, W. Y., *in* "Proceedings, 7th International Congress on Catalysis, Tokyo, 1980" (T. Seiyama and K. Tanabe, Eds.), p. 1047. Elsevier, Amsterdam, 1981.

35. Konishi, Y., Sakata, K., Misono, M., and Yoneda, Y., *J. Catal.* **77**, 169 (1982).

36. Neumann, R., and Levin, M., *J. Org. Chem.* **56**, 5707 (1991).

37. Minisci, F., Fontana, F., Araneo, S., Recupero, F., Banfi, S., and Quici, S., *J. Amer. Chem. Soc.* **117**, 226 (1995).

38. Sorokin, A., Robert, A., and Meunier, B., *J. Am. Chem. Soc.* **115**, 7293 (1993).

39. Nagano, T., Arakane, K., and Hirobe, M., *Chem. Pharm. Bull.* **28**, 3719 (1980).

40. Khenkin, A. M., and Shilov, A. E., *New J. Chem.* **13**, 659 (1989).

41. Lindsay Smith, J. R., and Sleath, P. R., *J. Chem. Soc. Perkin Trans. II*, 1165 (1983).

42. Neumann, R., and Khenkin, A. M., *Chem. Commun.*, 2643 (1996).

43. Balkus, K. J., Eissa, M., and Levado, R., *J. Amer. Chem. Soc.* **117**, 10753 (1995).

44. Sun, H., Blatter, F., and Frei, H., *J. Amer. Chem. Soc.* **118**, 6873 (1996).

45. Adam, W., Haas, W., and Lohray, B. B., *J. Am. Chem. Soc.* **113**, 6202 (1991).

46. Ballistreri, F. P., Tomaselli, G. A., Tuscuno, R. M., Conte, V., and Furia, F. D., *J. Am. Chem. Soc.* **113**, 6209 (1991).

47. Howarth, O. W., *Prog. NMR Spectrosc.* **22**, 453 (1990).

48. Neumann, R., and de la Vega, M., *J. Mol. Catal.* **84**, 93 (1993).